Detection of Pulmonary Fibrosis with a Collagen-Mimetic Peptide

Isabella M. Borgula,[†] Sergey Shuvaev,[#,‡] Eric Abston,[‡,§] Nicholas J. Rotile,[‡]
Jonah Weigand-Whittier,[‡] Iris Y. Zhou,[‡] Peter Caravan,[#,‡,*] and Ronald T. Raines[†,*]

[†]Department of Chemistry, Massachusetts Institute of Technology, Cambridge, Massachusetts 02139, United States; [#]Department of Radiology, Massachusetts General Hospital, Boston, Massachusetts 02124, United States; [‡]Athinoula A. Martinos Center for Biomedical Imaging, The Institute for Innovation in Imaging, Massachusetts General Hospital and Harvard Medical School, 149 Thirteenth Street , Charlestown, Massachusetts 02129, United States; [§]Department of Thoracic Surgery, Massachusetts General Hospital, Boston, Massachusetts 02124, United States

*Emails: pcaravan@mgh.harvard.edu; rtraines@mit.edu

Content **Page**

Abbreviations Used

ACN, acetonitrile
CD, circular dichroism
CHCA, α-cyano-4-hydroxycinnamic acid
CI, compositional isomer
CMP, collagen-mimetic peptide
DCM, dichloromethane
DIC, *N*,*N*′-diisopropylcarbodiimide
DMF, dimethylformamide
DMSO, dimethyl sulfoxide
DOTA, 1,4,7,10-tetraazacyclododecane-1,4,7,10-tetraacetic acid
flp, (2*S*,4*S*)-4-fluoroproline
Fmoc, fluorenylmethyloxycarbonyl
Gly, glycine
Hyp, (2*S*,4*R*)-4-hydroxyproline
HPLC, high-performance liquid chromatography
HRCT, high-resolution computed tomography
id/cc, injected dose per cubic centimeter
IPF, idiopathic pulmonary fibrosis
MALDI–TOF MS, matrix-assisted laser desorption/ionization time-of-flight mass spectrometry
MR, magnetic resonance
PBS, phosphate-buffered saline
PET, positron emission tomography
PPII, polyproline type II
Pro or P, (2*S*)-proline
RLMR, right lung:muscle ratio
SEM, standard error of the mean
Ser or S, (2*S*)-serine
*t*Bu, *tert*-butyl
TEA, triethylamine
TFA, trifluoroacetic acid
TIS, triisopropylsilane

General Experimental Procedures

Reagents. Commercial chemicals were of reagent grade or better, and were used without further purification. FmocGlyOH and HOBt were from Chem-Impex International (Wood Dale, IL). FmocflpOH and FmocHyp(*t*Bu)OH were from OmegaChem (Saint-Romuald, Canada). FmocGly-loaded Wang resin was from MilliporeSigma (Burlington, MA). DIC and 4-methylpiperidine were from Oakwood Chemical (Tampa, FL). DOTA–NHS ester was from Macrocyclics (Plano, TX). Anhydrous DMSO, TIS, TFA, and PBS (product P3813) were from Sigma–Aldrich (St. Louis, MO). All other reagents were from Fisher Scientific (Hampton, NH).

Conditions. All procedures were performed at ambient temperature (~23 °C) and pressure (1.0 atm) unless indicated otherwise.

Peptide Synthesis—General

This section was adapted from Dones et al., 2019.[1] Peptides were synthesized with a Liberty Blue Automated Microwave Peptide Synthesizer from CEM (Matthews, NC). All peptides were synthesized following CEM standard methods for both microwave and coupling cycles. Standard solutions of DIC (0.5 M in DMF), OxymaPure (1 M in DMF), 4-methylpiperidine (20% v/v in DMF), and Fmoc-protected amino acids (0.2 M in DMF) were prepared for each synthesis.

Standard Microwave-Assisted Deprotection. The microwave was set to 155 W at 75 °C for 15 s, followed by 30 W at 90 °C for 50 s.

Standard Microwave-Assisted Coupling. The microwave was set to 170 W at 75 °C for 15 s, followed by 30 W at 90 °C for 225 s.

Standard Coupling Cycle. FmocGly-loaded Wang resin (1 equiv) was added to the CEM reaction vessel, and the resin was allowed to swell for 5 min in DMF. The Fmoc group was removed using the standard deprotection solution and the microwave-assisted deprotection methods described above. The resin was then washed (4×), and Fmoc-AA-OH (5 equiv) was added, followed by DIC (20 equiv) and OxymaPure (40 equiv). Standard microwave-assisted coupling was performed with additional Fmoc-protected amino acids, and the resin was washed (2×) and drained. When double-coupling was required, the cycle was repeated without the deprotection step.

Cleavage and Precipitation. After the final deprotection step, the resin was removed from the reaction vessel into a cleavage filter, washed with DCM (4×), and air-dried crude peptides were then cleaved from the resin using a cleavage cocktail composed of 2.5:2.5:95 H_2O/TIS/TFA for 2 h. Peptide mixtures were then filtered and precipitated in ice-cold diethyl ether (10×). The peptides were collected by centrifugation, the supernatants were decanted, and the solid peptide was dissolved in 5 mL of 70:30 H_2O/ACN. The solutions were frozen and lyophilized using a FreeZone benchtop instrument from Labconco (Kansas City, MO). The crude peptide mixture was then subjected to purification.

Purification. The crude peptide products were purified by preparative reversed-phased HPLC using a XSelect Peptide CSH C18 OBD Prep Column 130 Å, 5 µm, 19 mm × 250 mm from Waters (Milford, MA) and a 1260 Infinity II instrument (Agilent Technologies, Santa Clara, CA). Crude products were dissolved in the minimum amount of ACN and eluted with a linear gradient of 5–80% v/v ACN in H_2O containing TFA (0.1% v/v). After reviewing the initial chromatogram, the method was updated, if necessary. Chromatography fractions were analyzed by MALDI–TOF MS using a microflex LRF instrument and a CHCA matrix (Bruker, Billerica, MA). Fractions containing purified peptide were pooled, lyophilized, and analyzed with reversed-phase HPLC using a 1260 Infinity II instrument (Agilent Technologies) and EC 250/4.6 Nucleosil 100-5 C18 column (Macherey–Nagel, Düren, Germany).

Peptide Synthesis—Specific

Scheme S1. Synthetic Route to [^{68}Ga]Ga·DOTA–CMP

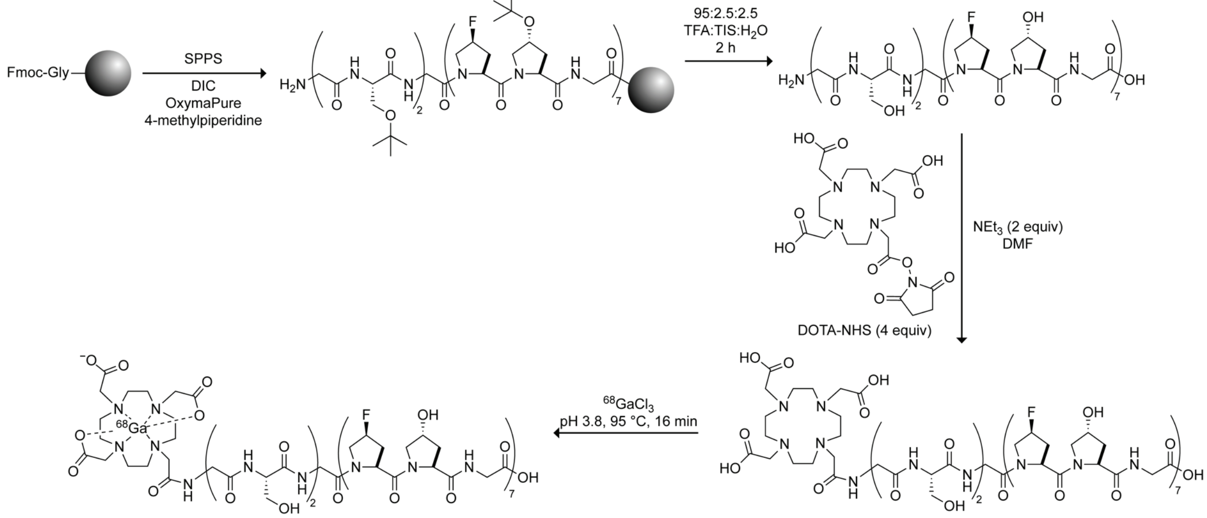

(Gly-Ser)$_2$-Gly-(flp-Hyp-Gly)$_7$ and (Gly-Ser)$_2$-Gly-(Hyp-flp-Gly)$_7$. Peptides were synthesized by a non-interrupted continuous method. After deprotection of FmocGly-loaded Wang resin, Fmoc-protected amino acids were coupled by either a single or a double standard coupling cycle until completion. The low nucleophilicity of flp and Hyp required a double standard coupling cycle. Following deprotection, the peptide was cleaved from the resin and precipitated to afford a crude peptide product. The crude product was purified with preparative reversed-phase HPLC, and chromatography fractions were analyzed by MALDI–TOF MS in positive-ion mode. Fractions containing pure material were pooled and lyophilized.

DOTA–(Gly-Ser)$_2$-Gly-(flp-Hyp-Gly)$_7$ and DOTA–(Gly-Ser)$_2$-Gly-(Hyp-flp-Gly)$_7$. The peptide was dissolved in DMF containing TEA (4 equiv), and the resulting solution was allowed to stir for 15 min. DOTA–NHS ester (2 equiv) was added to the mixture, and the resulting solution was allowed to react for 48 h. The reaction mixture was then concentrated under reduced pressure, diluted with water (5 equiv), frozen, and lyophilized. The peptide conjugate was purified with preparative reversed-phase HPLC, and chromatography fractions were analyzed by MALDI–TOF MS in positive-ion mode. Fractions containing pure material were pooled, and lyophilized. Purity was confirmed with analytical reversed-phase HPLC (Figure S1) and MALDI–TOF MS (Figure S2).

5(6)-TAMRA–(Gly-Ser)$_2$-Gly-(flp-Hyp-Gly)$_7$-NH$_2$. 5(6)-TAMRA–(Gly-Ser)$_2$-Gly-(flp-Hyp-Gly)$_7$-NH$_2$ was synthesized on low-loading Rink Amide Resin from CEM (product #R002), Fmoc-protected amino acids were coupled by either a single or a double standard coupling cycle until completion. The low nucleophilicity of flp and Hyp required a double standard coupling cycle. Following deprotection, the peptide was cleaved from the resin and precipitated to afford a crude peptide product. The crude product was purified with preparative reversed-phase HPLC, and chromatography fractions were analyzed by MALDI–TOF MS in positive-ion mode. Fractions containing pure material were pooled and lyophilized.

To conjugate the fluorophore, the peptide was dissolved in DMSO containing TEA (4 equiv), and the resulting solution was allowed to stir for 15 min. 5(6)-TAMRA–NHS ester (5 equiv) from Click Chemistry Tools (product #1074-1000) was added to the mixture, and the resulting solution was allowed to react overnight. The reaction mixture was then diluted with water, frozen, and lyophilized. The peptide conjugate was purified with preparative reversed-phase HPLC, and chromatography fractions were analyzed by MALDI–TOF MS in positive-ion mode. Fractions containing pure material were pooled, and lyophilized.

Circular Dichroism Spectroscopy

Peptides were dried under vacuum for ≥48 h before being weighed and dissolved to 0.8 mM in 50 mM acetic acid (pH 3.0). The resulting solutions were heated to 65 °C and cooled to 4 °C at a rate of 1 °C every 5 min. The solution was then incubated at ≤4 °C for ≥24 h before its CD spectrum was acquired with a Model J-1500 spectrometer (JASCO, Easton, MD) at the MIT Biophysics Instrumentation Facility. Spectra were measured with a bandpass of 1 nm. The signal was averaged for 3 s during the wavelength scan. Values of T_m were determined by fitting the molar ellipticity at 225 nm to a four-parameter Hill equation.

Radiosynthesis

[^{68}Ga]Ga·DOTA–CMP and [^{68}Ga]Ga·DOTA–CI. The following procedure was adapted from Désogère et al. (2017).[2] $^{68}GaCl_3$ in 0.1 M HCl was generated on demand with a ^{68}Ge/^{68}Ga generator from Eckert & Ziegler (Berlin, Germany). $^{68}GaCl_3$ [10 mCi, in 0.5 mL of HCl (0.6 M)] was purified by using a Sep-Pak C18 cartridge (Waters, Milford, MA) to remove any radiometal impurities (*e.g.*, ^{68}Ge breakthrough). An aliquot (150 µL) of the $^{68}GaCl_3$ solution was diluted with 100 µL of 1.5 M sodium acetate buffer, pH 4.5, to reach a pH of 4.0. A solution (100 µL) of 1 mg/mL DOTA–(GlySer)$_2$-Gly-(flp-Hyp-Gly)$_7$ or DOTA–(Gly-Ser)$_2$-Gly-(Hyp-flp-Gly)$_7$ in ultrapure water was added to the radioactive solution. The pH was checked and adjusted to ensure pH 4. The reaction mixture was heated to 95 °C for 15 min. After heating, the mixture was cooled for 2 min and radiochemical purity was assessed. The radiochemical purity of the final solution of DOTA–(Gly-Ser)$_2$-Gly-(flp-Hyp-Gly)$_7$ and DOTA–(Gly-Ser)$_2$-Gly-(Hyp-flp-Gly)$_7$ was ≥95%, as determined by radio-HPLC analysis (Figure S2) using an Agilent Technologies 1100 Series instrument, Carroll/Ramsey radiation detector with a silicon PIN photodiode and UV detection at 210 nm, a C18 column (150 mm × 4.6 mm) from Kromasil (Bohus, Sweden), and a linear gradient of 5–95% v/v ACN in H_2O containing TFA (0.1% v/v)]. The specific radioactivity was estimated to be ~1–3 GBq/µmol.

[^{64}Cu]Cu·DOTA–CMP and [^{64}Cu]Cu·DOTA–CI. $^{64}CuCl_2$ was obtained from the University of Wisconsin–Madison. An aliquot (100 µL) of $^{64}CuCl_2$ solution was diluted with 100 µL of 1.5 M sodium acetate buffer, pH 4.5. A solution (50 µL) of 1 mg/mL DOTA–(Gly-Ser)$_2$-Gly-(flp-Hyp-Gly)$_7$ or DOTA–(Gly-Ser)$_2$-Gly-(Hyp-flp-Gly)$_7$ in water was added to the radioactive solution. The reaction mixture was heated to 95 °C for 15 min. After heating, the mixture was cooled for 2 min and diluted with 650 µL of sterile water. Radiochemical purity was assessed with Radio-iTLC (BioScan AR2000). TLC was performed with an iTLC-SG paper (Agilent) stationary phase and a 50 mM EDTA, pH 5.0 mobile phase to facilitate detection of labile copper. The radiochemical purities of the final [^{64}Cu]Cu·DOTA–CMP and [^{64}Cu]Cu·DOTA–CI solutions were ≥95%.

Stability of CMP in Sera and Plasma

5(6)-TAMRA–(Gly-Ser)$_2$-Gly-(flp-Hyp-Gly)$_7$-NH$_2$. 5(6)-TAMRA–(Gly-Ser)$_2$-Gly-(flp-Hyp-Gly)$_7$-NH$_2$ was synthesized as described above. Human serum was obtained from Sigma–Aldrich (product #H4522); mouse serum was obtained from Thermo Fisher Scientific (product #10410). For all serum stability studies, 29 µM solutions of fluorophore conjugates in 50 mM HEPES–

NaOH buffer, pH 7.4, were prepared. Aliquots (600 μL) of the conjugate solutions were mixed with 400 μL of human serum or mouse serum, giving a final conjugate concentration of 21 μM. As a control, 600 μL of the conjugate solutions were mixed with 400 μL of 50 mM HEPES–NaOH buffer, pH 7.4. The samples were then incubated at 37 °C for 1 h after which and at appropriate time points, 50 μL of each sample was mixed with 50 μL of 0.2 M AcOH in CH_3CN. The resulting mixture was subjected to centrifugation at 13,000 rpm for 10 min. The supernatant was then isolated and stored at −20 °C for up for to 2 days prior to measurement. The stability of these peptides was analyzed with reversed-phase HPLC traces (λ = 557 nm).

[^{64}Cu]Cu·DOTA–CMP. An aliquot (50 μL) of [^{64}Cu]Cu·DOTA–CMP in PBS (1.0 mg/mL) was added to 300 μL of human plasma (MGH blood bank). The resulting mixture was incubated at 37 °C. At known times, an aliquot (50 μL) of this mixture was diluted with 250 μL of PBS containing EDTA (50 mM), and the resulting solution was analyzed with Radio-iTLC (BioScan AR2000).

Quantification of Hydroxyproline

An hydroxyproline assay kit from Sigma–Aldrich (product SKU MAK008-1KT) was used to quantify hydroxyproline in tissues. Tissues were homogenized using an immersion homogenizer prior to using the assay according to the manufacturer's instructions.

Animal Protocols

All experiments and procedures were performed in accordance with the "Guide for the Care and Use of Laboratory Animals" from the National Institutes of Health and were approved by the Massachusetts General Hospital Institutional Animal Care and Use Committee.

Animal Lung Fibrosis Model

In the bleomycin model, pulmonary fibrosis was induced in 6- to 8-week-old male C57/BL6 mice (Charles River Laboratories, Wilmington MA) by administering a single intratracheal dose of bleomycin (Fresenius Kabi, Lake Zurich, IL) (1.0 unit/kg), prepared in sterile PBS (50 μL). Sham mice were intratracheally injected with PBS. After 13 to 14 days after bleomycin (or PBS) instillation, animals were used for biodistribution and PET-MR imaging.

Animal PET-MR Imaging and Analysis

Mice were imaged in a 4.7 Tesla MRI scanner equipped with a PET insert (Bruker, Billerica, MA). Mice were anesthetized with isoflurane (4% for induction, 1–1.5% for maintenance in medical air). After placement of a tail-vein catheter for probe administration, mice were positioned in a prone position on a custom-built multi-animal cradle, which allows to image up to 4 mice at a time. Animals were kept warm with an air heater system with the temperature and respiration rate monitored by a physiological monitoring system (SA Instruments, Stony Brook, NY) throughout the imaging session. [^{68}Ga]Ga·DOTA–CMP or [^{68}Ga]Ga·DOTA–CI (100–200 μCi) was given intravenously as a bolus and followed by a 50-μL saline flush. MRI and PET acquisition were performed simultaneously. Anatomic MR images were acquired with a 3D Fast Low Angle Shot (FLASH) sequence [repetition time (TR)/echo time (TE)/flip angle (FA) = 20 ms/3 ms/12°, field of view (FOV) = 86 × 65 × 50 mm, 0.25 mm isotropic resolution]. Dynamic PET data were acquired in list-mode for up to 60 min after probe injection and were reconstructed using maximum likelihood expectation maximization (MLEM) algorithm with 12 iterations, 0.75 mm isotropic voxels, and binned into sequential time frames with durations of 9 × 20 s, 7 × 60 s, 6 × 300 s, 2 ×

600 s. Static PET data was acquired in list-mode for 30 min, 30 min after probe injection, and were reconstructed using maximum likelihood expectation maximization (MLEM) algorithm with 12 iterations, 0.75 mm isotropic voxels, and binned into sequential time frames with durations of 6 × 300s. Reconstructed PET data were analyzed with the AMIDE software package.[3] Volumes of interest (VOIs) over renal cortex, bladder, liver, myocardium, and skeletal muscle were defined on MR images and used for quantifying radioactivity of each organ/tissue. Results were expressed as percentage of injected dose per cubic centimeter of tissue (%ID/cc) and lung-to-heart ratio.

Ex Vivo Tissue Analysis

Adapted from Désogère et al. 2017[2] and Wahsner et al. 2019.[4] The left lung, blood, urine, heart, liver, left rectus femoris muscle, spleen, small intestine, kidneys, tail, gall bladder, and left femur bone were collected from all animals. These organs were weighed and radioactivity in each tissue was measured on a Wizard2Auto Gamma counter (PerkinElmer, Waltham, MA). Tracer distribution is presented as %ID/gram for all organs. The radioactivity in the left lung is likewise reported as %ID/lung. Following gamma counting, the left lung was homogenized for hydroxyproline quantification with a colorimetric assay. The right lung was inflated and fixed in neutral 10% buffered formalin, embedded in paraffin, and sectioned into 5 μm-thick slices for hematoxylin and eosin (H&E) and Picrosirius red staining. Picroirius red-stained slides were scanned, and images were digitally acquired with a Nanozoomer slide scanner (Hammamatsu Photonics, Shizuoka, Japan).[5,6]

Individual Animals in Study: Summary

A total of 24 C57/BL6 mice were used in this study.

A. Intratracheal bleomycin instillation imaged after 14 days (n = 5), all mice injected with [^{68}Ga]Ga·DOTA–CMP.
B. Intratracheal PBS instillation as sham control (n = 6), all mice injected with [^{68}Ga]Ga·DOTA–CMP.
C. In a paired study, 13 mice received intratracheal bleomycin instillation and were imaged after 13–14 days. On day 13, all mice were treated with [^{68}Ga]Ga·DOTA–CMP and imaged. On day 14, all mice were treated with [^{68}Ga]Ga·DOTA–CI and imaged.

All animals were sacrificed 90 min after injection for analysis ex vivo.

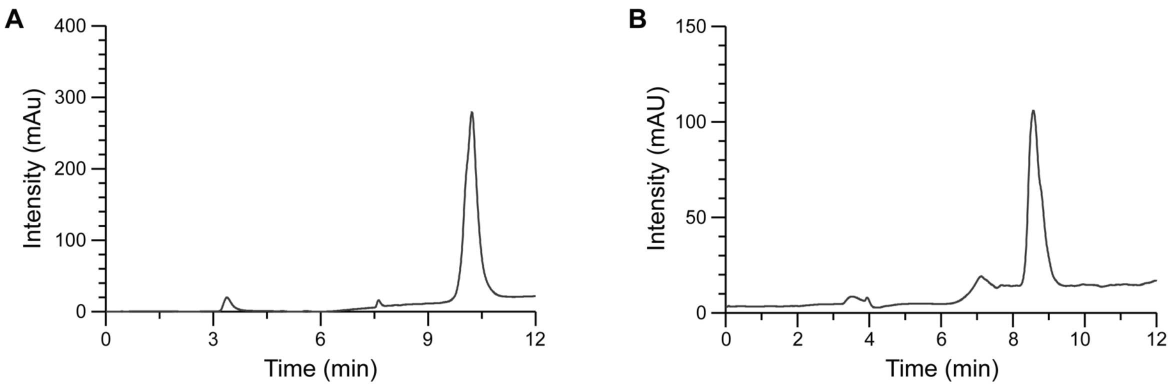

Figure S1. (A) Analytical HPLC trace of DOTA–CMP. (B) Analytical HPLC trace of DOTA–CI. Gradient: 0–70% v/v ACN in H_2O containing TFA (0.1% v/v) over 12 min.

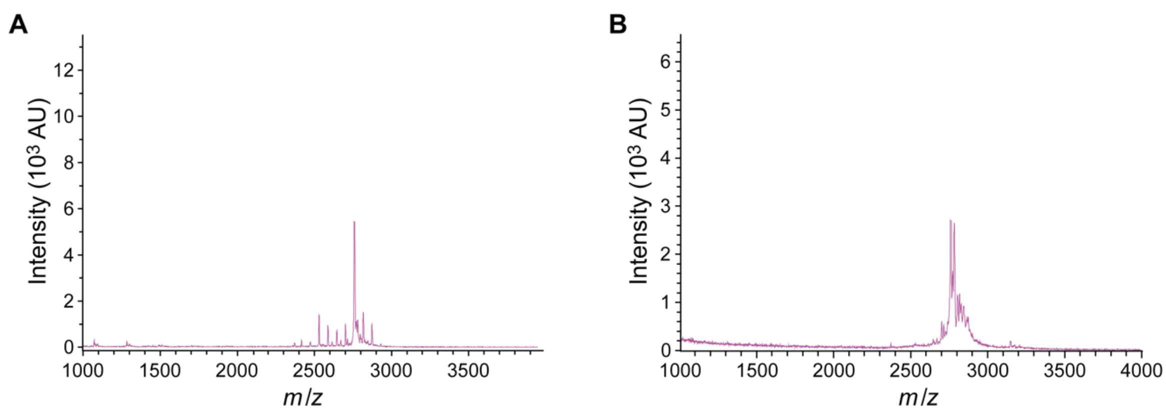

Figure S2. (A) MALDI–TOF mass spectrum of DOTA–CMP. $[M + H]^+$ (DA) calculated, 2747.67; found, 2747.80. $[M + Na]^+$ (DA) calculated, 2769.65; found, 2769.75. (B) MALDI–TOF mass spectrum of DOTA–CI. $[M + H]^+$ (DA) calculated, 2747.67; found, 2747.30. $[M + Na]^+$ (Da) calculated, 2769.65; found, 2769.64.

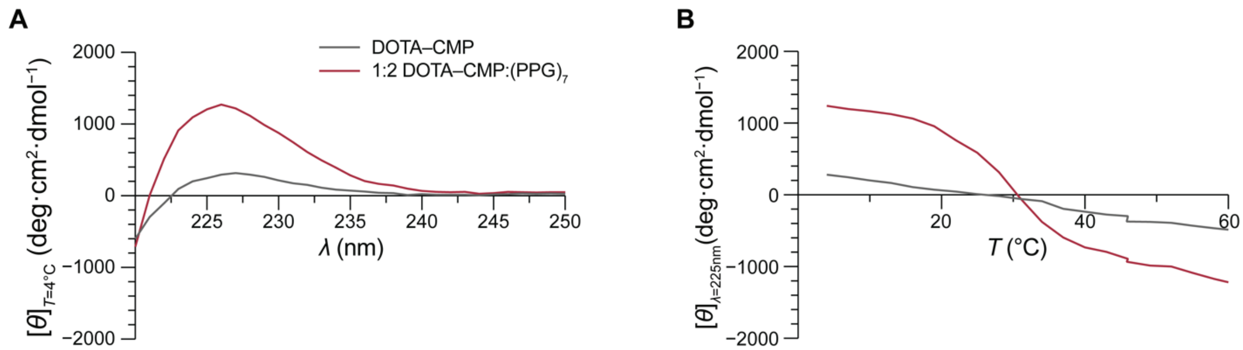

Figure S3. Analysis of DOTA–CMP or a 1:1 mixture of DOTA–CMP and $(PPG)_7$ with circular dichroism (CD) spectroscopy. Each solution contained 0.8 mM CMP (or a mixture) in 50 mM acetic acid. (A) Spectra of DOTA–CMP or a 1:1 mixture of DOTA–CMP and $(PPG)_7$ at 4 °C. (B) Melting curves of a 1:2 mixture of DOTA–CMP and $(PPG)_7$, and pure DOTA–CMP. DOTA–CMP alone does not demonstrate any cooperative denaturation, suggesting a lack of triple-helical structure. The 1:2 mixture undergoes cooperative denaturation with a T_m = 31 °C as determined by fitting to a 4-parameter Hill equation.

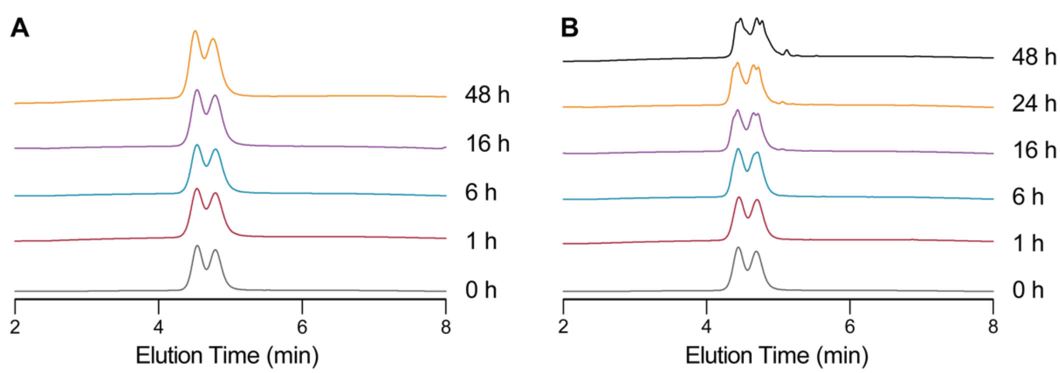

Figure S4. Reversed-phase HPLC traces (λ = 557 nm) showing the stability of 5(6)-TAMRA–$(Gly\text{-}Ser)_2$-Gly-$(flp\text{-}Hyp\text{-}Gly)_7$-$NH_2$ in 40% v/v serum and 60% v/v 50 mM HEPES–NaOH buffer, pH 7.4, at 37 °C. (A) Human serum. (B) Mouse serum. The two peaks derive from the two TAMRA isomers.

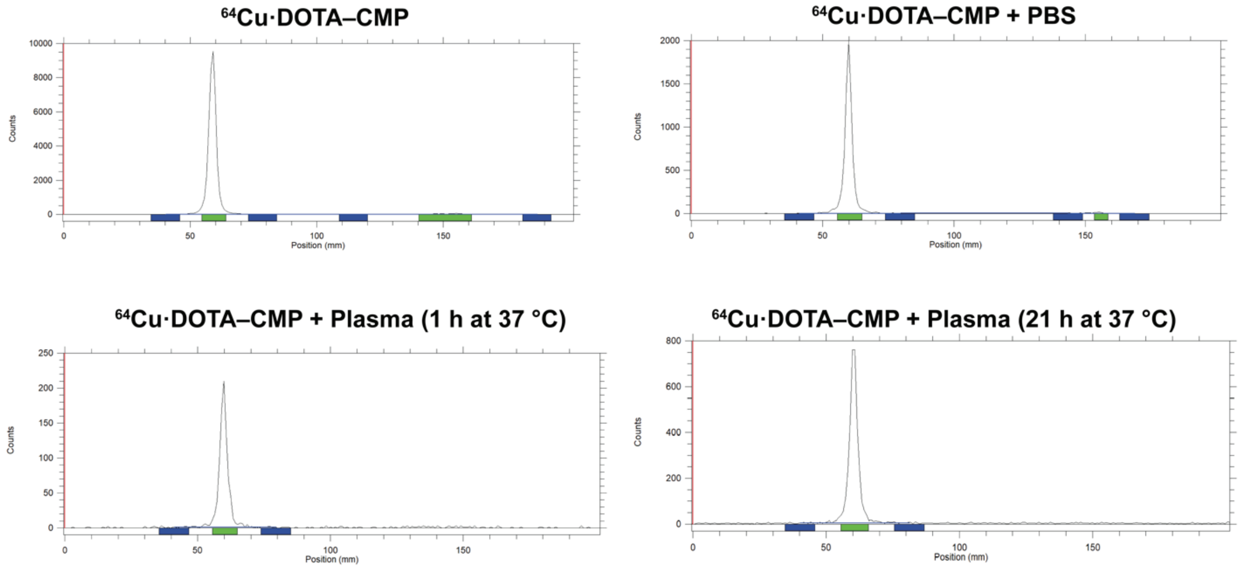

Figure S5. Radio-iTLC traces showing the stability of purified [^{64}Cu]Cu·DOTA–CMP incubated in PBS or human plasma for the stated time. No probe degradation was detectable under any condition.

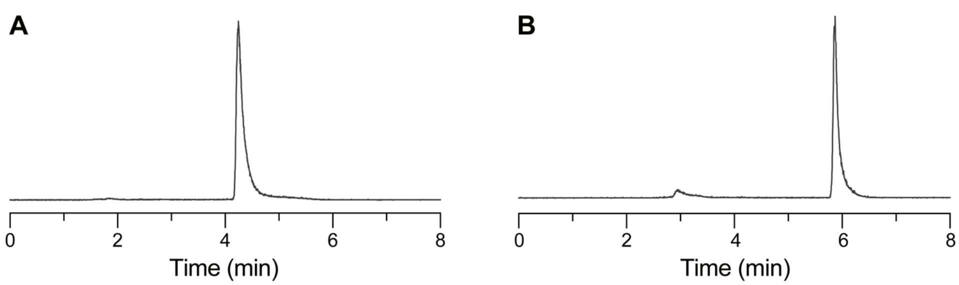

Figure S6. Radio-HPLC traces showing the radiochemical purity of [^{68}Ga]Ga·DOTA–CMP (A) and [^{68}Ga]Ga·DOTA–CI (B). Gradient: 0–100% v/v ACN in H_2O containing TFA (0.1% v/v) over 10 min.

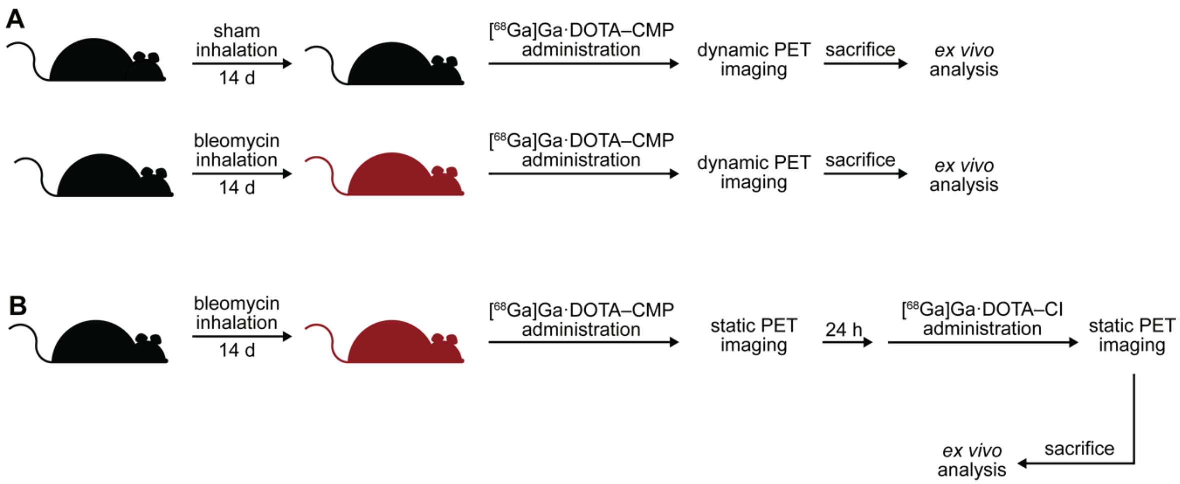

Figure S7. Design for in vivo and ex vivo experiments. (A) Basis for the data shown in Figure 3 and 4A, 4B, 4E, and 4F. (B) Basis for the data shown in Figures 4C and 4D.

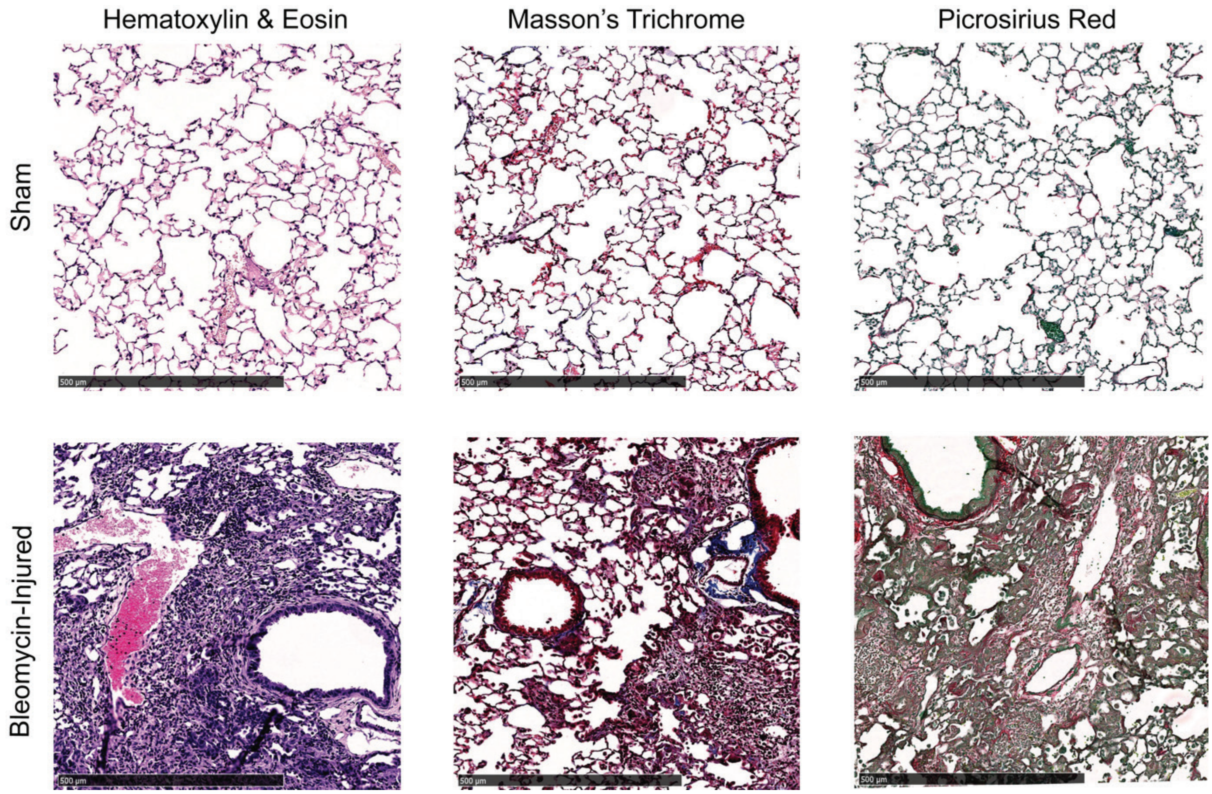

Figure S8. Representative images of right lung tissue stained with hematoxylin and eosin, Masson's trichrome, or Picrosirius red. Tissue samples from bleomycin-injured mice were collected 14 days after instillation of bleomycin. Scale bars, 500 μm.

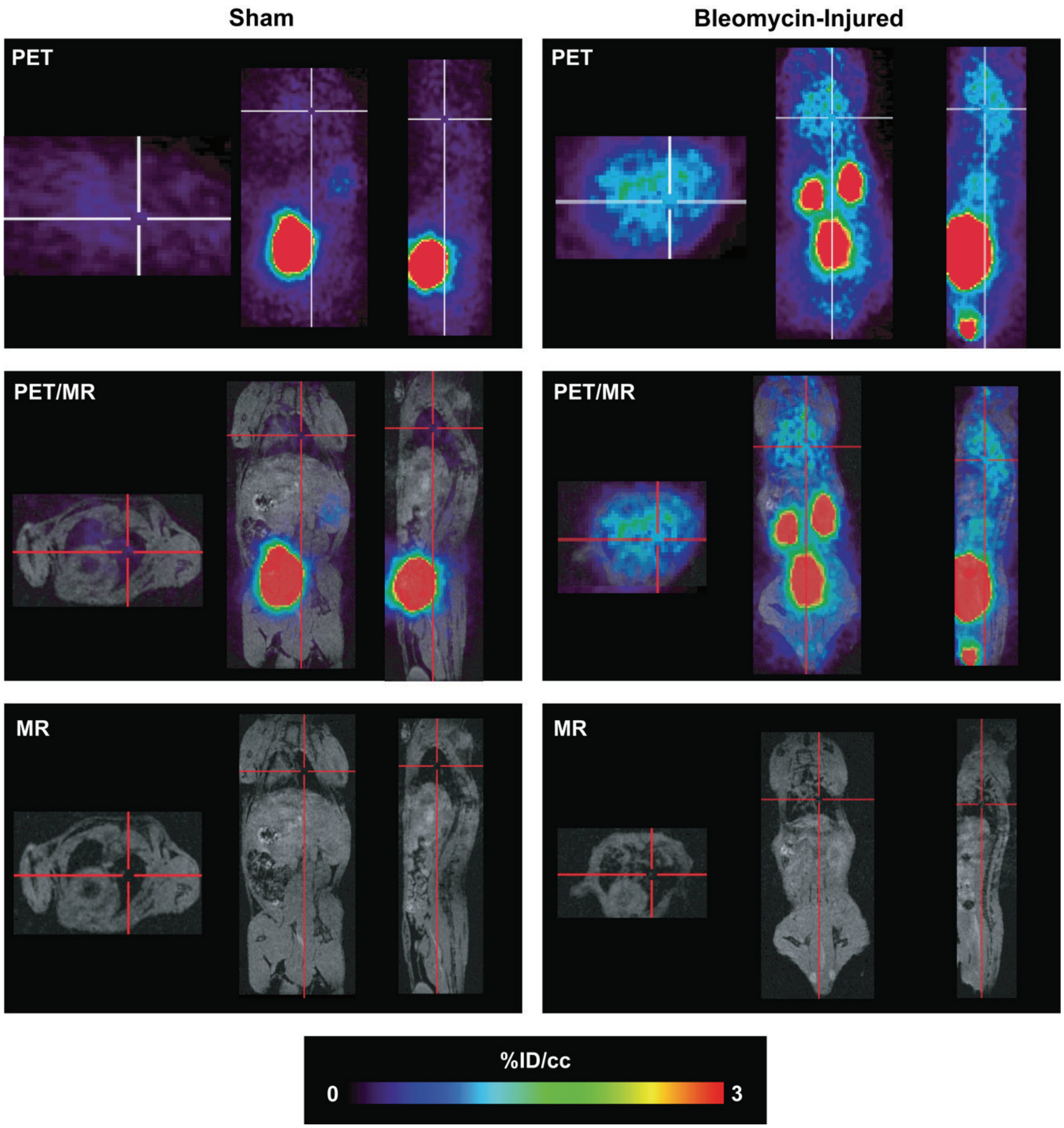

Figure S9. Representative images of sham and bleomycin-injured mice in either PET, fused PET/MR, or MR images as axial, coronal, or sagittal projections 50–60 min post-injection. The cross-hairs indicate the planes where images were taken. Grayscale images show MR image; color scale images show PET image. The color scale gives the injected radioactive dose per cubic centimeter of tissue (%ID/cc).

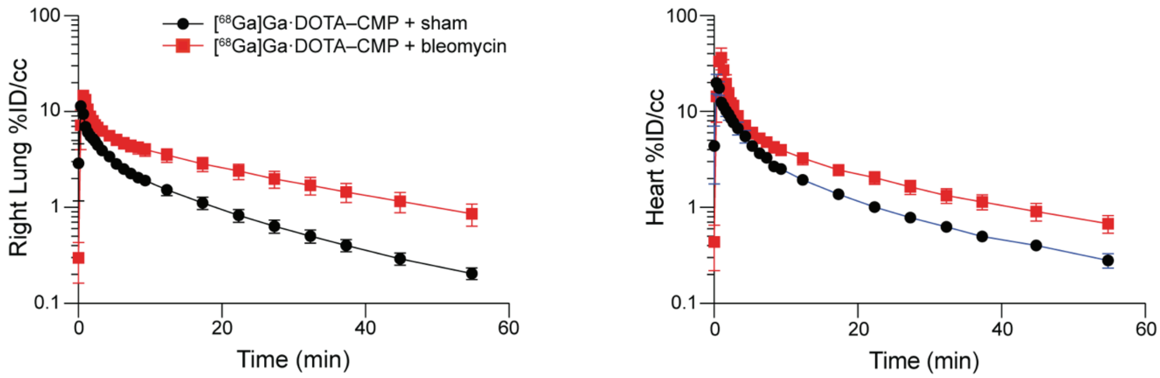

Figure S10. Time–activity curves for the right lung and heart for sham and bleomycin-injured mouse models of IPF. Values are the mean ± SEM. n = 6 for sham mice; n = 5 for bleomycin-injured mice.

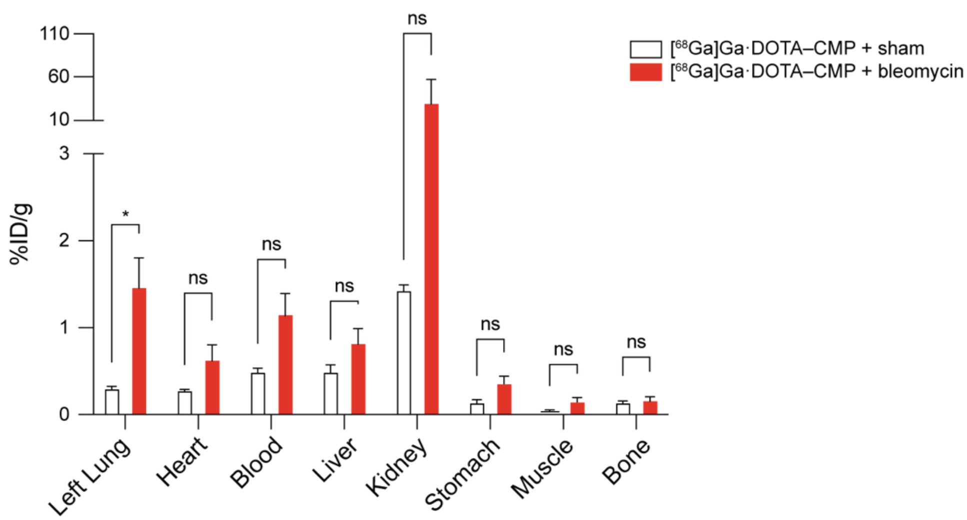

Figure S11. Ex vivo biodistribution data of [^{68}Ga]Ga·DOTA–CMP. Data were obtained by gamma-counting individual organs 90 min post-injection. Values are the mean ± SEM. Data were analyzed by using one-way ANOVA, followed by post hoc Tukey tests with a two-tailed distribution. *, $P < 0.1$; ns, not significant. For [^{68}Ga]Ga·DOTA–CMP + sham, n = 6. For [^{68}Ga]Ga·DOTA–CMP + bleomycin, n = 5.

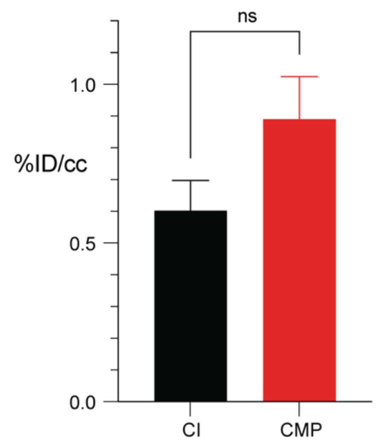

Figure S12. *In vivo* uptake of [^{68}Ga]Ga·DOTA–CMP and [^{68}Ga]Ga·DOTA–CI in the right kidney of bleomycin-injured mice 60 min post-injection. Data were obtained from the paired cohort in which mice were injected first with [^{68}Ga]Ga·DOTA–CMP, and then with [^{68}Ga]Ga·DOTA–CI 24 h later (Figure 7B). A paired *t*-test was performed on these data and indicated no significant difference ($P = 0.0878$) for the uptake of [^{68}Ga]Ga·DOTA–CMP and [^{68}Ga]Ga·DOTA–CI, $n = 9$.

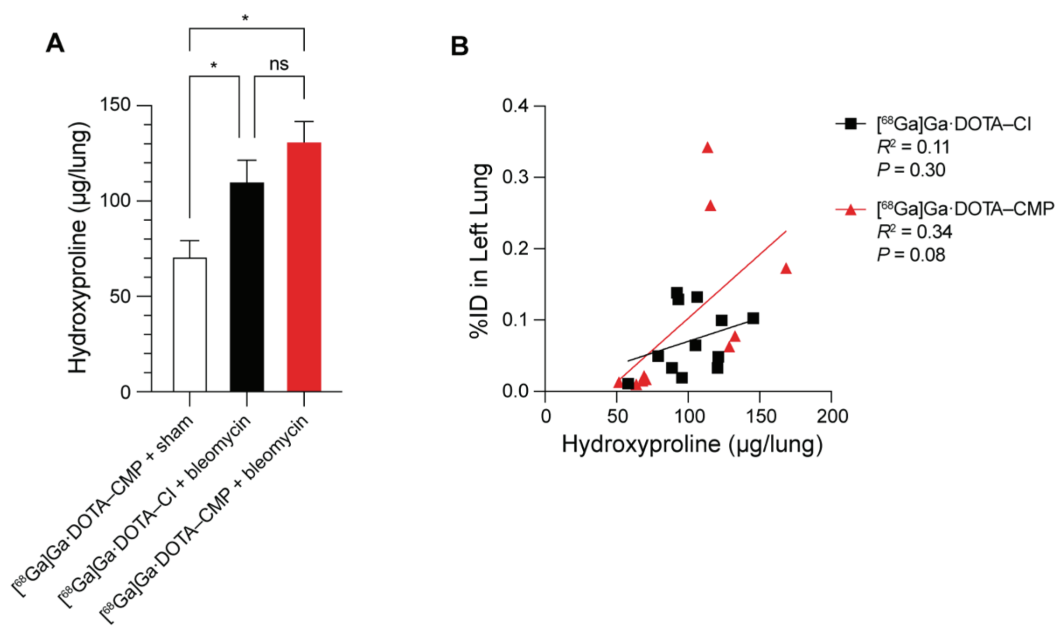

Figure S13. Relationship between [^{68}Ga]Ga·DOTA–CMP and [^{68}Ga]Ga·DOTA–CI uptake and hydroxyproline content. Hydroxyproline mass serves as a proxy for total collagen content, as this proline derivative is found almost exclusively in collagen. (A) Left lung hydroxyproline content as quantified by colorimetric quantification of tissue hydroxyproline. ns, not significant; *, $P < 0.1$. For [^{68}Ga]Ga·DOTA–CMP + sham, $n = 6$. For [^{68}Ga]Ga·DOTA–CI + bleomycin, $n = 13$. For [^{68}Ga]Ga·DOTA–CMP + bleomycin, $n = 5$. (B) Left-lung hydroxyproline content did not correlate well with ex vivo [^{68}Ga]Ga·DOTA–CMP or [^{68}Ga]Ga·DOTA–CI.

References

(1) Dones, J. M.; Tanrikulu, I. C.; Chacko, J. V.; Schroeder, A. B.; Hoang, T. T.; Gibson, A. L. F.; Eliceiri, K. W.; Raines, R. T. Optimization of interstrand interactions enables burn detection with a collagen-mimetic peptide. *Org. Biomol. Chem.* **2019**, *17*, 9906–9912.

(2) Désogère, P.; Tapias, L. F.; Hariri, L. P.; Rotile, N. J.; Rietz, T. A.; Probst, C. K.; Blasi, F.; Day, H.; Mino-Kenudson, M.; Weinreb, P.; Violette, S. M.; Fuchs, B. C.; Tager, A. M.; Lanuti, M.; Caravan, P. Type I collagen–targeted PET probe for pulmonary fibrosis detection and staging in preclinical models. *Sci. Transl. Med.* **2017**, *9*, eaaf4696.

(3) Loening, A. M.; Gambhir, S. S. AMIDE: A free software tool for multimodality medical image analysis. *Mol. Imaging* **2003**, *2*, 131–137.

(4) Désogère, P.; Tapias, L. F.; Rietz, T. A.; Rotile, N.; Blasi, F.; Day, H.; Elliott, J.; Fuchs, B. C.; Lanuti, M.; Caravan, P. Optimization of a collagen-targeted PET probe for molecular imaging of pulmonary fibrosis. *J. Nucl. Med.* **2017**, *58*, 1991–1996.

(5) Chen, H. H.; Waghorn, P. A.; Wei, L.; Tapias, L. F.; Schühle, D. T.; Rotile, N. J.; Jones, C. M.; Looby, R. J.; Zhao, G.; Elliott, J. M.; Probst, C. K.; Mino-Kenudson, M.; Lauwers, G. Y.; Tager, A. M.; Tanabe, K. K.; Lanuti, M.; Fuchs, B. C.; Caravan, P. Molecular imaging of oxidized collagen quantifies pulmonary and hepatic fibrogenesis. *JCI Insight* **2017**, *2*, e91506.

(6) Akam, E. A.; Abston, E.; Rotile, N. J.; Slattery, H. R.; Zhou, I. Y.; Lanuti, M.; Caravan, P. Improving the reactivity of hydrazine-bearing MRI probes for in vivo imaging of lung fibrogenesis. *Chem. Sci.* **2019**, *11*, 224–231.